THM COUPLING SENSITIVITY ANALYSIS IN GEOLOGICAL NUCLEAR WASTE STORAGE

Fabrice Dupray[1], **Chao Li**[1], **and Lyesse Laloui**[1]

[1] École Polytechnique Fédérale de Lausanne (EPFL)
School of Architecture, Civil and Environmental Engineering (ENAC)
Laboratory for Soil Mechanics (LMS) GC Station 18 1015 Lausanne, Switzerland
fabrice.dupray@epfl.ch, chao.li@epfl.ch, lyesse.laloui@epfl.ch

Keywords: nuclear waste storage, geomechanics, THM couplings, bentonite, EBS

Abstract. *A deep geological repository involving a multi-barrier system constitutes one of the most promising options to isolate high-level radioactive waste from the human environment. In order to certify the efficiency of waste isolation, it is essential to understand the behaviour of the confining geomaterials under a variety of environmental conditions. The efficiency of an Engineered Barrier System (EBS) is largely based on the complex behaviour of bentonite. To contribute to a better understanding of the processes involved in the EBS, a case study for sensitivity analysis has been defined and is studied using a thermo-hydro-mechanical (THM) finite element approach including a consistent thermo-plastic constitutive model for unsaturated soils. The model also features a coupled THM approach of the water retention curve. Various couplings were studied separately and in combination in order to determine the significance of each. The same principle is applied to physical phenomena such as vapour diffusion. This study clearly highlights the effects that need to be taken into consideration for a correct assessment of EBS behaviour.*

1 INTRODUCTION

The fate of high-level radioactive waste is of a great importance to nuclear power plants operators and government agencies responsible for safety due to their extremely slow decay and the high risks associated with their management. Geological disposal is widely regarded as the safest option to alleviate any undue burden for future generations caused by this type of radioactive material (IAEA, 2006). This idea led to the development of the Engineered Barrier System (EBS) principle, which consists of using different layers of protection to insulate radioactive waste in all situations, from the short-term high-temperature situation to the very-long term scenario. Such a radioactive waste design makes use of a carefully chosen natural barrier (the so called *host rock*, even if host clays are also planned), as well as two additional layers of protection. One of these is the canister that contains the waste, which is fabricated from a metal, such as pure copper or a specific steel alloy. The second layer of protection is a buffer material that is designed to dissipate heat in a controlled manner in order to mitigate the risks from movements of the drift (host rock fracturation, seismic events) and to limit the possibility of radionuclide migration.

The aim of this paper is to identify the various couplings, identified from laboratory-scale experiments, that are the most relevant to a full-scale EBS. The analysis takes into account both the evolution of the physical processes and the physical quantities relevant for the design of the EBS. The paper focuses on the behaviour of the buffer material, as this is the location of the most complex and physically coupled thermo-hydro-mechanical phenomena. The buffer material most commonly used in EBS designs is bentonite, either compacted as blocks or in pellet form (Karnland et al., 2011; NAGRA, 2002). Although they behave differently, these two forms of bentonite share a large number of their main characteristics (Laloui et al., 2008); they both exhibit a very low permeability, a highly variable thermal conductivity, an initial unsaturated state, and swelling characteristics.

The various processes that occur in the buffer are first outlined, with an emphasis on the coupled phenomena, as well as the necessary constitutive equations that describe them. This section includes the diffusive aspects (thermal and hydraulic behaviour), as well as their coupling using a mechanical constitutive model. Next, the chosen mechanical constitutive model is described, which is the ACMEG-TS model (François and Laloui, 2008), an elasto-thermoplastic model that uses the framework of generalized effective stress for unsaturated soils. In the second section, a case study is described that is designed to represent a generic EBS design with limited site effect, in order to underline the constitutive variations. This case study is simulated using the described constitutive equations in a finite element code. The results obtained for a base case are presented. Finally, results from a sensitivity analysis, with coupled phenomena turned on or off and with coupling parameter variations, are shown.

The case study under consideration is that of a single canister enclosed in a hole that is excavated without access drift. This choice allows the elimination of the site effects due to the drift and gives a better analysis of the effects of the modelling modifications. The geometry and heat dissipation are based on the Swedish proposal for an EBS (Karnland et al., 2011), and the canister emits heat according to the decay of a real high-level waste canister. The geometry of the vertical deposition hole is shown in Figure 1. As in the planned repositories, holes are excavated with a regular pattern, 400 m below the surface; therefore the modelled host rock radius is small (8.74 m) while a sufficient height is needed to avoid boundary effects (100 m).

2 COUPLED PROCESSES IN AN EBS

2.1 Physical description

With the exception of the canister, the materials involved in the problem are porous media. The description of diffusive processes in such media have been treated with a variety of approaches such as the theory of mixtures (Bowen, 1982), which is used here. This approach separates species and phases into constituents for the mass balance equations, allowing a clear identification of the phase change quantity, which cancel out in the balance equations of the chemical species, using the compositional approach (Collin et al., 2002; Panday and Corapcioglu, 1989). The diffusive model presented in section 2.2 is used for both the host rock and bentonite buffer.

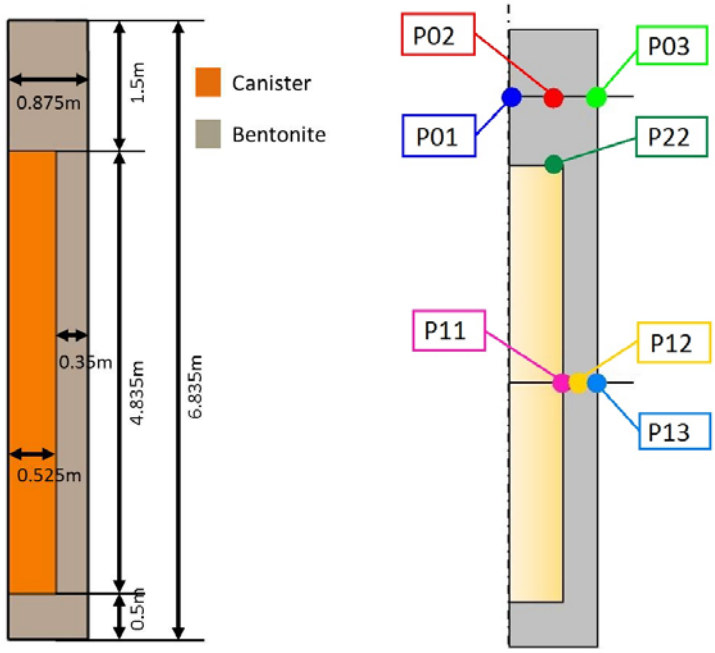

Figure 1: Geometry of the considered deposition hole, location of monitoring points.

In order to understand the various processes involved, it is necessary to define the extreme conditions that are encountered. The temperatures considered in this study are between 15 and 80 °C, which is the design criteria for some EBSs (Karnland et al., 2011). Higher temperatures up to 100 °C have been shown to increase the significance of vapour transport without introducing additional phenomena (Dupray et al., 2013). The host rock is considered to be saturated, and acts as a permanent supply of water to the initially unsaturated buffer. The first two processes are thus an increase in temperature adjacent to the canister (diffusion of decaying radionuclide heat) and water exchange at the boundary between the saturated host rock and unsaturated buffer materials. The heat generated is thought to be capable of provoking further drying of the unsaturated buffer, as well as vaporisation of water. In terms of modelling, this implies that the water retention model should be able to reproduce the effect of temperature on the retention capacity.

Changes in liquid water content strongly influence the thermal conductivity, as well as the heat capacity, of the porous media. Bentonite is extremely affected by this phenomenon (Börgesson et al., 2001). The degree of saturation will have a huge effect on the gas and liquid relative permeabilities of the porous medium. The diffusion of vapour created close to the canister should also be modelled, while the Richards' approximation is used to model vapour

diffusion in a static gas phase; Wang *et al.* (Wang et al., 2011) demonstrated the use of this solution to provide good results in full-scale simulations. Convective heat flow can also be induced by fluid flows and should be taken into account, for both vapour and liquid water.

Another aspect that influences the diffusive behaviour of the buffer is the effect that mechanical changes (strains) have on both water flow and thermal behaviour. The thermal behaviour is affected by density changes during compaction or dilation, while volumetric strains affect the intrinsic permeability of the buffer material. On the other hand, water migration in the media can be affected by changes in permeability caused by mechanical strains. When talking of a clayey material such as bentonite, this interpretation is not the only one possible and the concept of film transport, which depends on temperature and water content may also be used (Yong et al., 2010). This aspect is neglected here due to the small range of validity of this concept (from 10 to 20 % degree of saturation according to Winterkorn (1960)).

Thermo-hydro-mechanical couplings not only affect the diffusive part of the model, but also the mechanical one. The most well-known effects are the increase in strength that is induced by drying, and the changes in the swelling behaviour at high temperatures (Villar and Lloret, 2004). These experimentally-observed effects are taken into account directly in the constitutive model and are detailed in section 2.3.

2.2 Coupled diffusive model

2.2.1. Water species

As stated previously, the compositional approach is used, as implemented by Collin *et al.* (Collin et al., 2002) in the software *Lagamine*, that is also used for this study (Charlier et al., 2001). This approach allows writing the mass balance equation for water in a straightforward manner, including terms for storage of both liquid and gaseous water, advective flow of water, non-advective flow of vapour and source terms:

$$\underbrace{\frac{\partial}{\partial t}\left(\rho_w n S_r\right) + div\left(\rho_w \mathbf{f_l}\right) - Q_w}_{\text{Liquid water}} + \underbrace{\frac{\partial}{\partial t}\left(\rho_v n\left(1-S_r\right)\right) + div\left(\mathbf{i_v}\right) - Q_v}_{\text{Water vapour}} = 0 \tag{1}$$

where ρ_w and ρ_v are the bulk density of liquid water and water vapour; $\mathbf{f_l}$ is the macroscopic velocity of the liquid phase; $\mathbf{i_v}$ is the non-advective flux of water vapour, itself the opposite of dry air flux; S_r is the degree of liquid saturation, and n the porosity. The term $\rho_w n S_r$ is the storage term for liquid water. No gas flow appears, as per Richards' approximation.

Among these terms, the liquid water flow is defined by the generalized Darcy's law for porous media:

$$\mathbf{f_l} = -\frac{k_{r,w} k_{int}}{\mu_w} \mathbf{grad}\left(p_w\right) \tag{2}$$

where p_w is the liquid water pressure, $k_{r,w}$ the relative permeability to water, k_{int} the intrinsic permeability and μ_w the dynamic viscosity of liquid water. The relationship between the relative permeability and degree of saturation is defined according to the properties of each material. The intrinsic permeability depends on porosity through a Kozeny-Carman relationship:

$$k_{int} = k_{int,0}\left[\frac{n/n_0}{(1-n)/(1-n_0)}\right]^{\eta} \tag{3}$$

where $k_{int,0}$ is the intrinsic permeability at the initial porosity n_0 and η is a material parameter. This relationship and the storage term in equation (1) define one side of the hydro-mechanical coupling.

As the vaporisation/condensation term is not visible in the compositional approach, the thermo-hydraulic coupling does not appear as such in these relationships, and should be highlighted separately as appearing in several terms of equation (1). One element of this coupling is the evolution of the water properties with temperature, such as liquid density, but also dynamic viscosity. The dynamic viscosity of water is calculated through the relationship proposed by Thomas and King (Thomas and King, 1994), which is valid for the range of temperatures considered here:

$$\mu_w = 0.6612(T-229)^{-1.562} \tag{4}$$

where μ_w is the dynamic viscosity of water in Pa.s and T the temperature in Kelvin.

Liquid water is treated as a compressible and dilatant fluid, which is a correct assumption between 10 and 100 °C. The linearized relationship for the definition of liquid density is:

$$\rho_w = \rho_{w0}\left[1+\kappa_T(p_w - p_{wr}) - \beta_w(T-T_r)\right] \tag{5}$$

where κ_T is the isothermal water compressibility, β_w the volumetric thermal expansion coefficient of water and p_{wr} and T_r are the reference pressure and temperature, respectively.

The effect of temperature on water is more important when considering vapourization. It is interesting here to define the matrix suction as the difference between the gas pressure and (negative) water pressure, as $s=p_g-p_w$ (otherwise, when $p_w<p_g$, $s=0$). Vapour in the porous medium is supposed to be in thermodynamical equilibrium with liquid water, and, using Kelvin-Laplace's law as the definition of relative humidity h, the following relationship is obtained:

$$\rho_v = \rho_{v,sat}h = \rho_{v,sat}\exp\left(\frac{-s}{\rho_w R_v T}\right) \tag{6}$$

where R_v is the gas constant of water vapour, and $\rho_{v,\mathrm{sat}}$ is the saturated vapour density, that is itself dependent on temperature. This relationship is used in the vapour diffusion law that is based on Fick's law in a tortuous medium:

$$\mathbf{i_v} = -D\tau n(1-S_r)\,\mathbf{grad}(\rho_v) \tag{7}$$

where $\mathbf{i_v}$ is the vapour flow, D is the diffusion coefficient and τ the tortuosity.

It is then possible to distinguish the terms linked to the water pressure gradient from those linked to the temperature gradient in the gradient of vapour density, assuming the gradient of liquid water density is negligible:

$$\mathbf{grad}(\rho_v) = -\frac{\rho_v}{\rho_w R_v T}\mathbf{grad}(s) + \left[\frac{\rho_v}{\rho_{v,sat}}\frac{\partial\rho_{v,sat}}{\partial T} + \frac{\rho_v s}{\rho_w R_v T^2}\right]\mathbf{grad}(T) \tag{8}$$

This relationship shows the ability of the model to reproduce the transport of water vapour caused independently by suction and temperature gradients.

2.2.2. Heat diffusion

The energy balance equation of the mixture has the following form (Collin et al., 2002):

$$\underbrace{\frac{\partial H}{\partial t}+L\frac{\partial}{\partial t}\left(\rho_v n\left(1-S_r\right)\right)}_{\text{Heat storage}}+\underbrace{div\left(\mathbf{f_T}\right)+L\cdot div\left(\mathbf{i_v}\right)}_{\text{Heat transfer}}-Q_T=0 \tag{9}$$

where H is the enthalpy of the whole medium, L the latent heat of water vaporization, $\mathbf{f_T}$ the heat flow and Q_T the volume heat source. Due to the assumption of thermal equilibrium, a single temperature is defined for solid, liquid and gas phases. The enthalpy can then be defined as the sum of the heat of each constituent:

$$H=\left[\left(1-n\right)\rho_s c_{p,s}+nS_r\rho_w c_{p,w}+n\left(1-S_r\right)\rho_v c_{p,v}+n\left(1-S_r\right)\rho_a c_{p,a}\right]\left(T-T_r\right) \tag{10}$$

where ρ_s is the soil grain bulk density and $c_{p,w}$ $c_{p,s}$, $c_{p,a}$ and $c_{p,v}$ are the specific heat of liquid water, solid, dry air and water vapour, respectively. Heat transport is governed by conduction and convection:

$$\mathbf{f_T}=-\lambda\mathbf{grad}\left(T\right)+\left[c_{p,w}\rho_w\mathbf{f_l}+\left(c_{p,v}-c_{p,a}\right)\mathbf{i_v}\right]\left(T-T_0\right) \tag{11}$$

where λ is the thermal conductivity of the mixture. Depending on the properties of each material, this physical characteristic is either considered as a function of the volume ratios of solid, liquid water and gas phases, or a specific function for the material. This distinction allows consideration of the specific evolution of bentonite thermal conductivity in relation to its degree of saturation.

In terms of couplings, it can be observed that both thermo-hydraulic and thermo-mechanical couplings are present through the evolution of the variables n and S_r.

2.3 Coupled mechanical constitutive model

2.3.1. Stress-strain framework

The mechanical part of the model that is used to describe the behaviour of the buffer in this study, ACMEG-TS – Advanced Constitutive Model for Environmental Geomechanics – has already been the subject of papers by François and Laloui. (François and Laloui, 2008) and Dupray *et al.* (Dupray et al., 2013). The reader is advised to turn to these papers for a more detailed overview of the model. Since focus of this paper is thermo-hydro-mechanical coupling, only the related aspects of the model are detailed in this section.

The behaviour of the solid matrix is assumed to be governed by the generalized effective stress tensor $\boldsymbol{\sigma'}$ through a combination of total stress and fluid pressures (Laloui and Nuth, 2009):

$$\boldsymbol{\sigma'}=\boldsymbol{\sigma}-p_g\mathbf{I}+S_r\left(p_g-p_w\right)\mathbf{I} \tag{12}$$

The term ($\boldsymbol{\sigma}$-$p_g\mathbf{I}$) is called the net stress, while (p_g-p_w) is the matrix suction s. The Lagrangian approach is used in the model, with the small strain deformation theory. The importance of using the generalized effective stress theory is to encompass most effects of suction in a single equation (Nuth and Laloui, 2008b), which is important in hydro-mechanical coupling.

An important part of the thermo-mechanical coupling lies in the definition of strain, due to the phenomenon of thermal expansion. The following description of thermo-elasto-plastic strains is used:

$$d\boldsymbol{\varepsilon} = \mathbf{E}^{-1} d\boldsymbol{\sigma}' + \frac{\beta_s}{3}\mathbf{I}dT + d\boldsymbol{\varepsilon}^{\mathbf{p}} \tag{13}$$

where $d\boldsymbol{\varepsilon}$ is the total strain tensor increment, $\mathbf{E}$ the current non-linear elastic tensor, β_s the volumetric thermal expansion coefficient and $d\boldsymbol{\varepsilon}^{\mathbf{p}}$ the plastic strain tensor increment. The role of possible plastic strains on a thermal loading path where $d\boldsymbol{\sigma}'$ is null is evident in this equation. An important feature that derives from equations (12) and (13) is the behaviour during a suction decrease at constant volume and constant temperature, or the unsaturated isothermal swelling pressure test path, which is described by this relation:

$$d\boldsymbol{\sigma} = -d(S_r s)\mathbf{I} - \mathbf{E}d\boldsymbol{\varepsilon}^{\mathbf{p}} \tag{14}$$

It can be noted that in the absence of plastic strains, the development of swelling pressure depends entirely on the increment of the product of suction and degree of saturation. This highlights the mechanical influence of the choice of the water retention behaviour. It also shows that along a complete swelling pressure loading path, the manner in which plastic strains develop is also critical to the description of the swelling pressure development. Together with the influence of suction and temperature on the plastic behaviour, which have been treated in detail in (Cekerevac and Laloui, 2004; François and Laloui, 2008; Hueckel et al., 2009), these constitute the most intricate elements of the thermo-hydro-mechanical coupling.

2.3.2. Water retention behaviour

The water retention behaviour that is used in this study aims at representing at best the couplings observed in experiments on bentonite rather than focusing on a better representation of a one-directional wetting or drying path. It has been observed that temperature has a measurable effect on the relationship between the degree of saturation and suction, inducing a decrease in the degree of saturation for a constant suction (Romero et al., 2001). The effect of dry density changes, which are linked to volumetric strain, is also well-known (Gallipoli et al., 2003; Nuth and Laloui, 2008a). A complete water retention behaviour model should also include the hysteresis between drying and wetting paths.

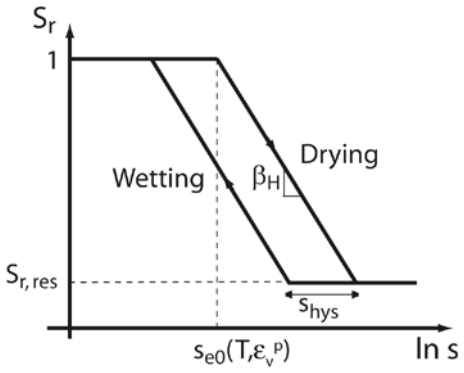

Figure 2: Schematic representation of water retention modelling

The water retention model is shown in Figure 2.Two different yield limits in the (S_r–s) plane are activated depending on the direction of the loading, as long the suction is higher than the air entry value:

$$\begin{cases} f_{dry} = s - s_d = 0 \\ f_{wet} = s_{hys} s_d - s = 0 \end{cases} \tag{15}$$

where s_d is the drying yield limit and s_{hys} the parameter describing the size of the hysteresis. The expression of the drying yield limit contains the coupled aspects of the formulation:

$$s_d = s_{e0} \exp\left(-\beta_h \ \Delta S_r\right)\left[1 - \theta_T \log\left(T/T_0\right) - \theta_e \log\left(1-\varepsilon_v\right)\right] \tag{16}$$

where s_{e0} is the initial air entry value of the saturated material, β_h the slope of the desaturation curve in the (S_r–s) plane at constant volume and temperature, θ_T and θ_e are material parameters describing the evolution of air-entry suction with respect to temperature and volumetric strain, respectively.

2.3.3. THM plastic formulation

It is beyond the scope of this paper to fully describe the plasticity model that is used here, which is given in François and Laloui (François and Laloui, 2008). As the swelling behaviour is fundamental in the response of the buffer of an EBS, only some elements of the isotropic behaviour will be analysed, emphasis on THM couplings. The coupling equation is based on the use of preconsolidation pressure as the main variable:

$$p'_c = \begin{cases} p'_{c0} \exp\left(\beta \ \varepsilon_v^p\right)\left[1 - \gamma_T \log\left(T / T_r\right)\right] & \text{if } s \le s_e \\ p'_{c0} \exp\left(\beta \ \varepsilon_v^p\right)\left[1 - \gamma_T \log\left(T / T_r\right)\right]\left[1 + \gamma_s \log\left(s / s_e\right)\right] & \text{if } s \ge s_e \end{cases} \tag{17}$$

where p'_{c0} is the saturated initial preconsolidation pressure at the reference temperature T_r; β is the plastic compressibility modulus, defined as $\beta = \beta_m + \Omega.s$ (β_m being the plastic compressibility in saturated conditions) and γ_T and γ_s are material parameters. Since the shape of the initial yield surface is defined by the value of the effective preconsolidation pressure, the isotropic part of the yield surface is well represented by this value. In Figure 3, the evolution of preconsolidation pressure with suction and temperature is represented. A decrease of this value with increasing temperature allows the creation of plastic strains in a purely thermal loading, thus representing the phenomenon of thermal collapse. A decrease in the suction will lead to the pressure reaching the yield surface, thus representing wetting collapse.

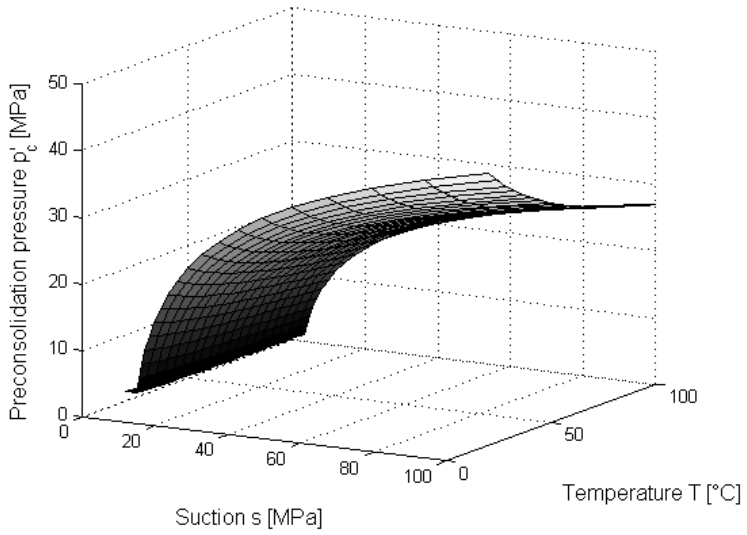

Figure 3: Effect of temperature and suction on preconsolidation pressure (or isotropic yield limit)

3 CASE STUDY CHARACTERISTICS

3.1 Material characteristics

It is necessary to describe the two materials in this case study: the host rock and the buffer material. The rock is modelled as granite, with the objective that it does not directly control the water supply to the unsaturated buffer, inducing a relatively high intrinsic permeability of 10^{-17} m2. The other characteristics, such as porosity, bulk and shear modulus, heat capacity, thermal conductivity are derived from both in situ and laboratory measurements (Maaranen et al., 2001; Makurat et al., 2006; Sundberg, 2002). The rock is initially saturated but comes in contact with a high suction material during the test. Therefore, it may desaturate and, through changes in relative permeability, influence the resaturation process. Based on the findings of Finsterle and Pruess (Finsterle and Pruess, 1995), a van Genuchten function is used to describe the retention behaviour of granite, and its associated function for relative permeability:

$$S_w = \left(1+\left(s / P_r\right)^{1/(1-m)}\right)^{-m} \tag{18}$$

$$k_{r,w} = \sqrt{S_w}\left(1-\left(1-S_w^{\,1/m}\right)^{m}\right)^{2} \tag{19}$$

where m and P_r are a material parameter and a reference pressure, respectively. Mechanically, the host rock is considered as a linear elastic material in the classical effective stress framework.

The buffer is made of highly compacted MX-80 bentonite blocks. These blocks have a saturated density of 2000 kg/m^3 (dry density 1517 kg/m^3). The initial degree of saturation is 0.61, corresponding to a suction of 48 MPa. A base case is considered, using parameters that are derived from those used by Åkesson et al. (2010) and adapted to the previously described constitutive model. Variations in some of the parameters are then considered to perform the analysis of THM couplings in the buffer. The parameters for the base case of the constitutive equations presented in sections 2.2 and 2.3 are summarized in Table 1. Some empirical relationships of the model were not treated directly as a part of the constitutive model and are

detailed here. The relative permeability description of the rock is crucial, and a power law is used (Vaunat and Gens, 2005):

$$k_{r,w} = S_w^{\ 3} \tag{20}$$

The specifics of the changes in bentonite thermal conductivity during changes in the degree of saturation also lead to the use of an empirical law that best describes the results gathered in (Åkesson et al., 2010):

$$\lambda = \lambda_{sat} - \frac{\lambda_2}{1+\exp\left((S_w - S_3)/S_4\right)} \tag{21}$$

where λ_{sat} is the saturated thermal conductivity, and λ_2, S_3 and S_4 are parameters for the relationship.

Table 1: Parameters used in the base case simulation for both bentonite and granite

Thermal parameter	Symbol	Unit	Bentonite	Granite
Saturated thermal conductivity	λ_{sat}	W/(m.°C)	1.3	-
Thermal conductivity parameter	λ_2	W/(m.°C)	1.04	-
"	S_3	-	0.52	-
"	S_4	-	0.12	-
Solid thermal conductivity	λ_s	W/(m.°C)	-	2.4
Water thermal conductivity	λ_w	W/(m.°C)	-	1.18
Air thermal conductivity	λ_a	W/(m.°C)	-	0
Solid heat capacity	$c_{p,s}$	J/(kg.°C)	800	770
Water heat capacity	$c_{p,w}$	J/(kg.°C)	4183	4183
Air heat capacity	$c_{p,a}$	J/(kg.°C)	1000	1000
Solid thermal expansion coefficient	β_s	K^{-1}	1.02×10^{-5}	2.16×10^{-5}
Water thermal expansion coefficient	β_w	K^{-1}	3.4×10^{-4}	3.4×10^{-4}
Flow parameter				
Intrinsic permeability	k_{int}	m^2	6.4×10^{-21}	1×10^{-17}
Kozeny-Carman parameter	η	-	5.33	-
Relative permeability parameter	m	-	-	0.6
Relative permeability parameter	P_r	MPa	-	1.74
Initial porosity	n_0	-	0.438	0.003
Tortuosity	τ	-	1	1
Other parameters				
Solid specific mass	ρ_s	kg/m^3	2780	2700
Water specific mass	ρ_w	kg/m^3	1000	1000
Air specific mass	ρ_a	kg/m^3	1.18	1.18
Isothermal water compressibility	κ_T	Pa^{-1}	0	0
Mechanical parameters				
Young's modulus	E	GPa	see Table 2	62
Poisson's ratio	ν	-	0.2	0.24

As stated earlier, the constrained swelling response of the buffer is crucial to the mechanical behaviour of the whole EBS design. The dry density of the buffer considered here leads to a design swelling pressure of 5.21 MPa. This value, along with the saturated elastic modulus of 20 MPa allows the determination of a set of parameters for the isothermal

unsaturated behaviour of the buffer in the ACMEG-TS model, as explained in (Dupray et al., 2013). These parameters are shown in Table 2.

Table 2: Set of ACMEG-TS parameters for the base case simulation (see (François and Laloui, 2008))

Elastic parameters		
K_{ref}, G_{ref}, n^e	[MPa], [MPa], [-]	22.2, 16.7, 1
Isotropic plastic parameters		
β, γ_s, γ_T, r^e_{iso}, p'_c, Ω	[-], [-], [-], [-], [MPa] , [-]	30, 8, 0.2, 0.7, 1.5, 10^{-6}
Deviatoric plastic parameters		
b, d, ϕ', g, α, a, r^e_{dev}	[-], [-], [°], [-], [-], [-], [-]	0.1, 2, 30, 0, 1, 0.001, 0.8
Water retention parameters		
s_{e0}, β_h, θ_T, θ_e, s_{hys}	[MPa], [-], [-], [-], [-]	3, 7, 0, 0, 0

3.2 Simulation characteristics

The model consists of 2211 8-node elements and is run as an axisymmetric model. Apart from the geometry of the problem that was defined in the introduction, it is necessary to describe the loading path of the simulation. The initial equilibrium is obtained by the application of forces along the empty hole. In a first stage, the considered hole is excavated by releasing those forces. A 100 % humidity rate is then applied in the hole for 30 days. The operational stage of the EBS is finally simulated through the introduction of a heat-emitting canister and its surrounding buffer material. The canister emits heat at an initial rate of 1700 W, with a progressive decay that can be seen in Table 3, derived from the work of Hökmark *et al.* (Hökmark et al., 2008). The canister itself, though not described previously, is modelled as a continuous material described by linear thermo-elasticity, with a Young's modulus of 180 GPa, a Poisson's ratio of 0.3 and a volumetric thermal expansion coefficient of 5.1×10^{-5} K^{-1}.

Table 3: Simulated heat decay of the canister

Time [yr]	Power [W]
0	1700
1	1671
10	1416
20	1232
50	828
100	520
1000	109

4 BASE CASE AND SENSITIVITY

4.1 Base case description

This section presents the values that will serve as a reference for the analysis of variations in the buffer behaviour. The chosen values are the maximum temperature, the maximum suction, the resaturation time and the swelling pressure. These values all correspond to a design criteria of EBS, and as such appear as the most relevant for a sensitivity analysis. They

are monitored at 7 locations as shown in Figure 1: three points are at the level of the middle of the canister, three are 75 cm above the canister and one is on top of the canister.

With regard to temperature, a value of 79 °C is reached 20 years after emplacement in location P22. The temperature evolution at all points is given in Figure 4, which shows the buffer effect of the bentonite gap in terms of maximum temperature and the corresponding time delay for points 75 cm above the canister. Figure 5 shows the evolution of pore pressure in the first years, mainly in the negative values (suction). The locations close to the canister are affected by an increase in suction, reaching more than 120 MPa on top of the canister and more than 60 MPa on the side, starting from 49 MPa. The evolution of the degree of saturation shown in Figure 6 is another sign of the same phenomenon, with the degree of saturation going below 0.5 at the top of the canister. The resaturation time is 4.1 years on the sides, but 5.3 years on the top. Finally Figure 7 and Figure 8 present the evolution of both the mean effective stress and mean mechanical stress (or swelling pressure), the swelling stress tensor being defined as $\boldsymbol{\sigma}_{sw} = \boldsymbol{\sigma}' + S_r s \mathbf{I}$. Two main effects are visible: drying shrinkage and final swelling pressure. Drying shrinkage is visible (as tensile net stresses) in the aforementioned areas close to the canister, most notably on top of it. Tensile stresses are obtained due to the perfect bonding that is assumed between elements in the simulation, used instead of modelling the gaps necessary for construction. This simplification may affect local results on top of the canister but does not significantly affect other factors of the simulation as the main real gap (between blocks and host rock) is quickly filled by swelling bentonite saturated from water inflow from granite. The final swelling pressure establishes itself between 5.2 and 6.9 MPa in all locations, highlighting the sealing capacity of the buffer. This is close to the design value of 5.25 MPa. The corresponding dry density variations during drying and/or swelling are in the order of 50 kg/m3, highest densities being seen close to the canister during drying shrinkage.

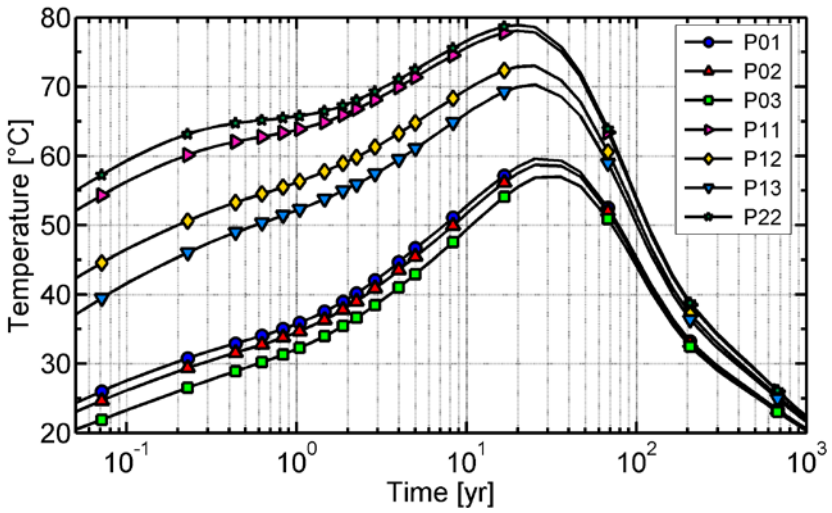

Figure 4: Temperature evolution in the base case

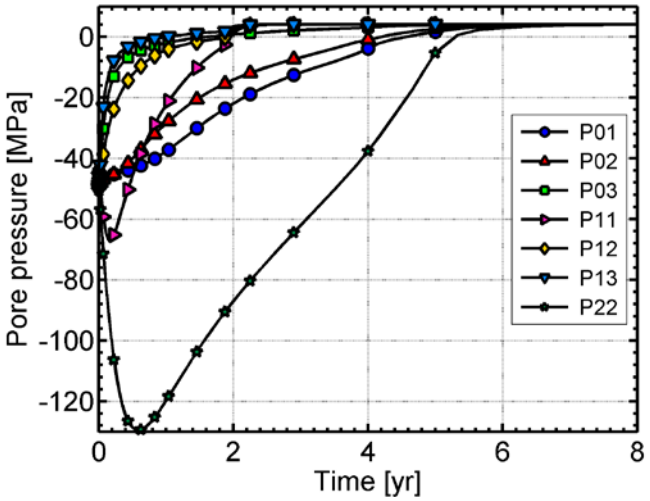

Figure 5: Pore water pressure evolution in the base case

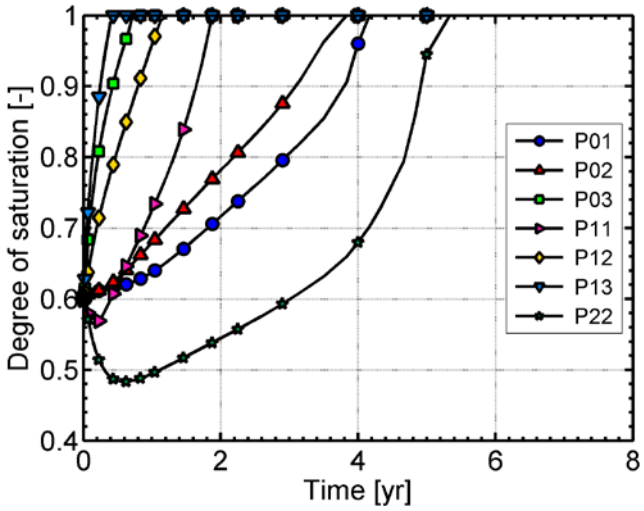

Figure 6: Degree of saturation evolution in the base case

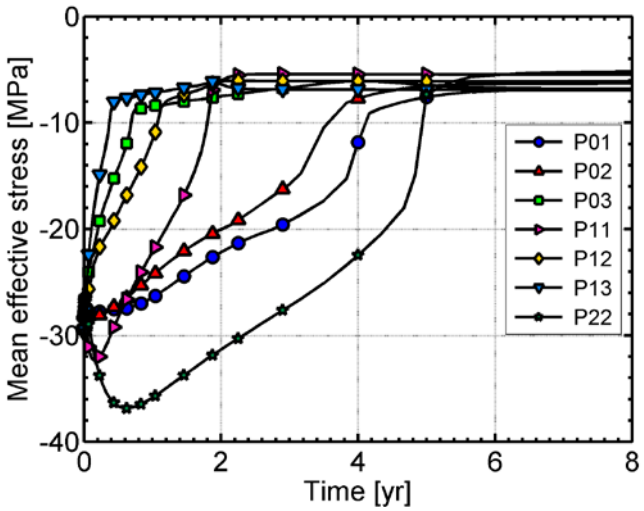

Figure 7: Mean effective stress evolution in the base case

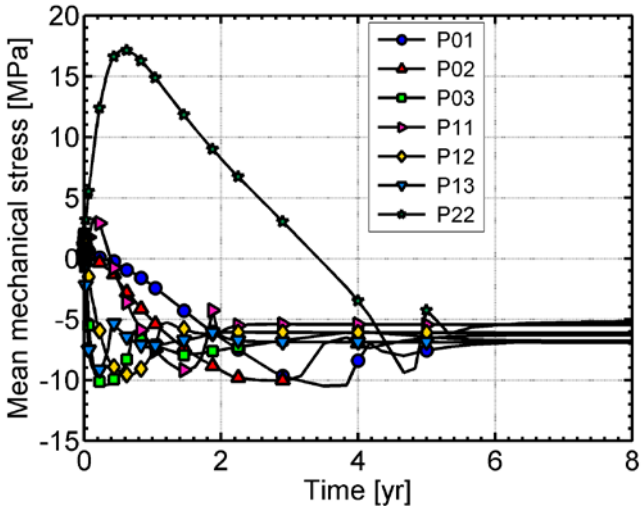

Figure 8: Swelling pressure evolution in the base case

4.2 Influence of physical processes

The first step of this analysis is to assess the pertinence of possible simplifications in the constitutive description of the diffusive part of the model. Two aspects are treated: the effect of vapour flow, and the effect of convective heat flow. Case 3-2 was run without vapour diffusion, or $\mathbf{i}_v=0$, although vapour is still created according to Kelvin-Laplace law. Case 3-6 was run without convective heat transport: eq. (11) is reduced to $\mathbf{f}_T=-\lambda\mathbf{grad}(T)$. Figure 9 highlights the strong effect of vapour diffusion in the resaturation process, even in the low temperature case that is considered here. All points exhibit a very different evolution of pore pressures between the two cases. In particular, no drying occurs in locations P11 and P22, and the resaturation process is much faster at the top of the canister. This shows how important the vapour diffusion process is for a correct representation of the resaturation process: instead of a continuous liquid water flow from the granite, there is a combination of this water flow and diffused vapour condensation that accelerates the process in most places, especially at the sides of the canister with its limited thickness. The acceleration is due to both the vapour transport and a faster increase of relative permeability, highlighting the thermo-hydraulic coupling. For pore pressures, case 3-6 and the base case give extremely similar results.

Figure 10 deals with the evolution of temperature in the three cases. Here the changes are much more limited, both in magnitude and in terms of the area involved. Only the buffer in the extreme vicinity of the canister is measurably influenced, with a deviation of -1.2 °C in the case 3-2 and +0.6 °C in case 3-6. The temperature decrease in case 3-2 is explained by the higher vapour pressures (up to 50 % more) encountered transitorily in the first year; this is because more energy is dissipated as latent heat of vaporisation. The temperature increase in case 3-6 simply measures the amount of heat that is transported by convective heat transport in vapour flow. It should be noted that temperature is otherwise largely unaffected by variations of the parameters not affecting Kelvin's law directly.

The conclusions of this section are that the need to include vapour diffusion in the model is shown to be fundamental in any EBS simulation and the need to take into account convective heat flow is more limited. While this seems unnecessary in the described situation, it may remain important to take it into account if the peak temperature of the EBS is reached while the buffer is still unsaturated.

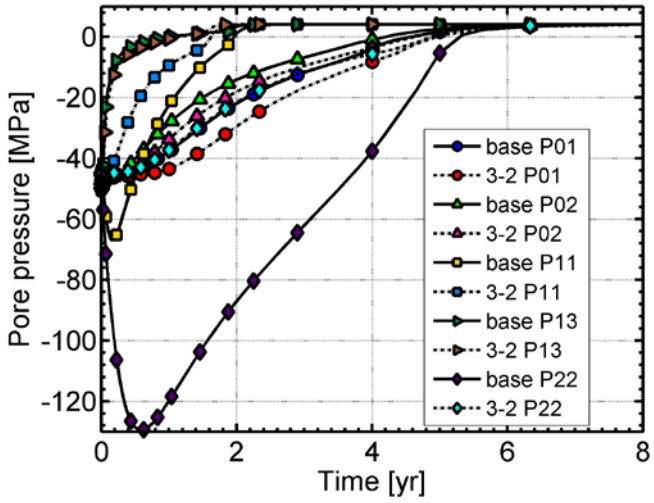

Figure 9: Evolution of pore water pressure in base case and case 3-2 for 5 locations

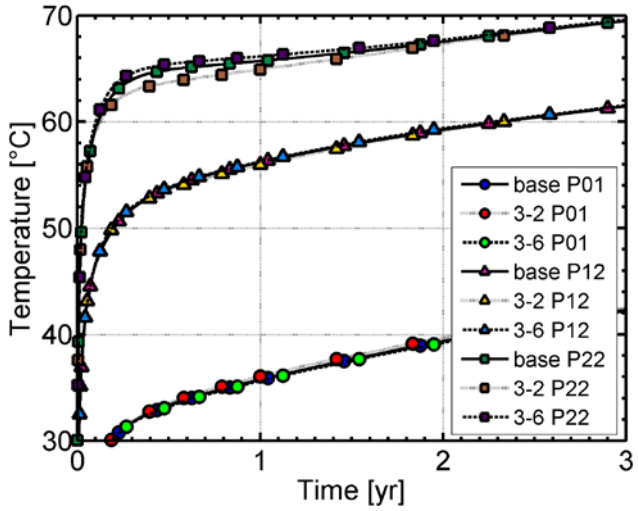

Figure 10: Evolution of temperature in base case, cases 3-2 and 3-6 for 3 locations

4.3 Influence of the water retention description of the buffer

Analysis of the constitutive model indicates that the water retention behaviour plays a major and central role in the THM couplings in an EBS. Acting directly on the hydraulic and mechanical parts (and, as a secondary effect, on the thermal part), water retention is directly influenced by all three aspects. The base case introduced the simplest description by neglecting all influences acting on the retention behaviour. Three influences are then introduced as separate cases: the effect of the hydraulic loading path is introduced as a hysteretic loop in the retention curve (case 5-1-2); the effect of temperature is introduced as case 5-2-1; and the effect of volume change is introduced as case 5-3-2.

In order to introduce the hysteretic water retention behaviour that is experimentally observed with bentonite but rarely seen in actual simulations, the initial water retention curve is set as the drying path. The parameter s_{hys} is set at 0.8. The effect of temperature is set by the parameter θ_T at 0.5, and finally the effect of volume changes by the parameter θ_e at 15. The effect of all these changes are seen in Figure 11, which shows the evolution of the degree of saturation with time in all four cases at two significant locations, highlighting both the

minimal degree of saturation and total time of resaturation. The mechanical influence is treated in the next section.

The effect of temperature on the retention behaviour is the most influential parameter and its effect on bentonite has been quantified by Villar and Lloret in experimental results (Villar and Lloret, 2004). For similar water contents, the ratio between the suction at 20 and 60 °C lies between 1.5 and 5. In this simulation, this same ratio can reach 4 for temperatures of 20 and 70 °C. The additional time needed to resaturate the buffer on top of the canister is more than 1 year, and 5 months on the side. The minimal degree of saturation is much lower than in the base case but the maximal suction is only 10 MPa more due to the effect that a temperature increase has on the water retention curve.

The effect of the hysteretic loop is the second most influential on the resaturation process. Its effect is obvious in the area that dries for the longest period (P22), where the plateau before wetting due to the hysteretic behaviour is obvious, Figure 11. The additional time to resaturation is 7 months on top of the canister, and 1.5 months on the side. Finally the effect of volumetric changes on the retention curve is the least influential in the case of an EBS. The bentonite buffer is in a confined environment and, although its swelling is inhomogeneous, it is not subject to extreme volume changes. The initial shrinkage in the locations considered limits desaturation slightly, but this trend reverses during the resaturation and swelling of bentonite, leading to a measurable but non-significant delay in resaturation.

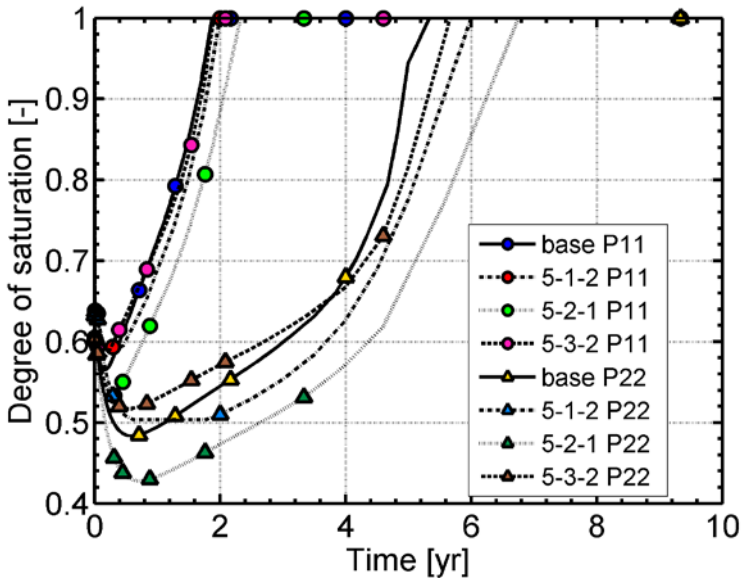

Figure 11: Evolution of degree of saturation with changes in the water retention behaviour

4.4 Influence of couplings on the mechanical response

For the thermal and hydraulic response, the main factors influencing the mechanical response – namely, the development of swelling pressure – are also investigated in this paper. Two cases from the preceding section were also analysed for this aspect, using the analysis of a parameter of the ACMEG-TS model, γ_T. This parameter, although specific to the ACMEG-TS model, is an indicator of the known behaviour of bentonite, i.e., thermally-induced plasticity. An indication of this behaviour can be found in the significant decrease in swelling pressure (from roughly 5 MPa to 2.5 MPa between 20° and 80 °C) that has been identified in (Villar and Lloret, 2004). An increase of this parameter γ_T from 0.2 to 0.5 is considered in case 5-4-1.

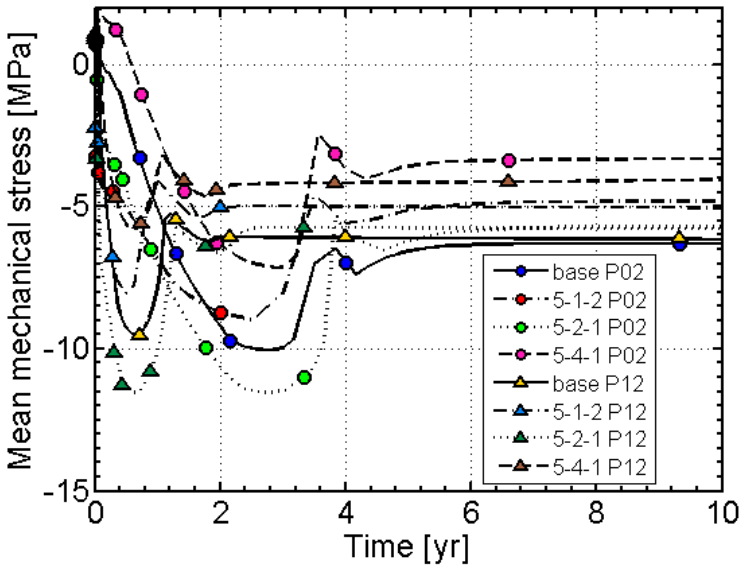

Figure 12: Evolution of swelling pressure in two central points for four cases

Figure 12 shows the development of swelling pressure in the base case as well as in the three most significant cases, in two locations, one on the side and one in the upper part of the buffer. This figure highlights the intrinsic coupling of water retention with swelling, as the introduction of both couplings (hysteresis and thermal coupling) leads to a measurable effect on the final swelling pressure. The thermal coupling decreases the final swelling by 0.4 MPa while a change in the wetting curve decreases it by 1.1 MPa.

Finally, the effect of the more direct thermo-mechanical-coupling parameter is logically more important. By increasing the possibility (smaller elastic surface) and the quantity of thermally triggered plastic strains, the model is able to reproduce the strong decrease in swelling pressure observed experimentally, with a 2.8 MPa decrease from the base case. This shows the pertinence of treating the effects of suction and temperature in the same framework, by allowing parameter identification from existing literature. Such a decrease is also very significant for the engineering of an EBS and to allow a correct description of design values, which are all too often given at ambient temperature, while the operation of the EBS will be at a higher temperature.

5 CONCLUSIONS

This paper investigates, through a sensitivity analysis, the importance of constitutive behaviour description and parameterisation in the global response of an EBS. Through a case study based on the Swedish design, with a maximum temperature of around 80 °C, various conclusions have been drawn. In terms of the representation of physical processes, the importance of the role of vapour creation and diffusion has been highlighted, even for low temperatures, while the role of convective heat transport has been deemed as significant only in particular cases. The importance of a correct description of water retention behaviour has been shown, especially with regards to the THM couplings. Only the coupling of retention behaviour with volumetric strain is seen as unnecessary in an EBS simulation, due to the stiff boundaries of the excavated hole. The effects of hysteresis and thermal coupling are both seen as significant, in terms of resaturation time, but also for the mechanical behaviour of the buffer. The swelling response of the buffer, which is shown to reproduce all the characteristics observed in the experiments, is influenced by the water retention behaviour and

also by the thermal coupling in the ACMEG-TS model. A description of the individual characteristics of the EBS design elements based on ambient temperature measurements is seen as inaccurate if the coupled effect of temperature is not taken into account. The paper shows how a thermally-coupled process in retention behaviour can have consequences, down to the swelling behaviour. The magnitude of the influence of these couplings is comparable to more studied parameters, such as buffer density, which are already recognized as important for an EBS design.

ACKNOWLEDGMENTS

The authors wish to thank NAGRA for the opportunity to work on this project and Prof. Charlier and Dr Collin(University of Liège) for their software *Lagamine*.

REFERENCES

Åkesson, M., Börgesson, L., Kristensson, O., 2010. SR-Site Data report: THM modelling of buffer, backfill and other system components, in: SKB TR-10-44, Technical Report. SKB, Stockholm, 98 p.

Börgesson, L., Chijimatsu, M., Fujita, T., Nguyen, T.S., Rutqvist, J., Jing, L., 2001. Thermo-hydro-mechanical characterisation of a bentonite-based buffer material by laboratory tests and numerical back analyses. Int. J. Rock Mech. Min. Sc. 38, 95-104.

Bowen, R.M., 1982. Compressible porous media models by use of the theory of mixtures. International Journal of Engineering Science 20, 697-735.

Cekerevac, C., Laloui, L., 2004. Experimental study of thermal effects on the mechanical behaviour of a clay. Int. J. Numer. Anal. Meth. Geomech. 28, 209-228.

Charlier, R., Radu, J.-P., Collin, F., 2001. Numerical modelling of coupled transient phenomena. Rev. Fr. Génie Civ. 5, 719-743.

Collin, F., Li, X.L., Radu, J.P., Charlier, R., 2002. Thermo-hydro-mechanical coupling in clay barriers. Eng. Geol. 64, 179-193.

Dupray, F., François, B., Laloui, L., 2013. Analysis of the FEBEX multi-barrier system including thermoplasticity of unsaturated bentonite. Int. J. Numer. Anal. Meth. Geomech. 37, 399-422.

Finsterle, S., Pruess, K., 1995. Solving the Estimation-Identification Problem in Two-Phase Flow Modeling. Water Resour. Res. 31, 913-924.

François, B., Laloui, L., 2008. ACMEG-TS: A constitutive model for unsaturated soils under non-isothermal conditions. Int. J. Numer. Anal. Meth. Geomech. 32, 1955-1988.

Gallipoli, D., Wheeler, S.J., Karstunen, M., 2003. Modelling the variation of degree of saturation in a deformable unsaturated soil. Géotechnique 53, 105-112.

Hökmark, H., Lönnqvist, M., Fälth, B., 2008. Rock Mechanics Issues in the Swedish Waste Management Program, The 42nd U.S. Rock Mechanics Symposium (USRMS). American Rock Mechanics Association, San Francisco, CA.

Hueckel, T., François, B., Laloui, L., 2009. Explaining thermal failure in saturated clays. Géotechnique 59, 197-212.

IAEA, 2006. International Atomic Energy Agency: Geological disposal of Radioactive Waste. Safety Requirements, No. WS-R-4, IAEA Safety Standards Series.

Karnland, O., Olsson, S., Sandén, T., Fälth, B., Jansson, M., Eriksen, T.E., Svärdström, K., Rosborg, B., Muurinen, A., 2011. Long term test of buffer material at the Äspö HRL, LOT project, in: SKB TR-09-31, Technical Report. SKB, Stockholm, 123 p.
Laloui, L., François, B., Nuth, M., Péron, H., Koliji, A., 2008. A thermo-hydro-mechanical stress-strain framework for modeling the performance of clay barriers in deep geological repositories for radioactive waste, 1st European Conf. on Unsaturated Soils, Durham, UK, pp. 63-80.
Laloui, L., Nuth, M., 2009. On the use of the generalised effective stress in the constitutive modelling of unsaturated soils. Comput. Geotech. 36, 20-23.
Maaranen, J., Lehtioksa, J., Timonen, J., 2001. Determination of porosity, permeability and diffusivity of rock samples from Äspö HRL using the helium gas method, in: SKB IPR-02-17, International Progress Report. SKB, Stockholm.
Makurat, A., Løset, F., Wold Hagen, A., Tunbridge, L., Kveldsvik, V., Grimstad, E., 2006. A descriptive rock mechanics model for the 380–500 m level, in: SKB R-02-11, Report. SKB, Stockholm.
NAGRA, 2002. Project Opalinus Clay: Safety Report. Demonstration of disposal feasibility (Entsorgungsnachweis) for spent fuel, vitrified high-level waste and long-lived intermediate-level waste, NTB 02-05, Technical Report. NAGRA, Wettingen, Switzerland.
Nuth, M., Laloui, L., 2008a. Advances in modelling hysteretic water retention curve in deformable soils. Comput. Geotech. 35, 835-844.
Nuth, M., Laloui, L., 2008b. Effective stress concept in unsaturated soils: Clarification and validation of a unified framework. Int. J. Numer. Anal. Meth. Geomech. 32, 771-801.
Panday, S., Corapcioglu, M.Y., 1989. Reservoir transport equations by compositional approach. Transport Porous Med. 4, 369-393.
Romero, E., Gens, A., Lloret, A., 2001. Temperature effects on the hydraulic behaviour of an unsaturated clay. Geotechnical and Geological Engineering 19, 311-332.
Sundberg, J., 2002. Determination of thermal properties at Äspö HRL, in: SKB R-02-27, Report. SKB, Stockholm, 66 p.
Thomas, H.R., King, S.D., 1994. A non-linear, two-dimensional, potential-based analysis of coupled heat and mass transfer in a porous medium. Int. J. Num. Meth. Eng. 37, 3707-3722.
Vaunat, J., Gens, A., 2005. Analysis of the hydration of a bentonite seal in a deep radioactive waste repository. Eng. Geol. 81, 317-328.
Villar, M.V., Lloret, A., 2004. Influence of temperature on the hydro-mechanical behaviour of a compacted bentonite. Appl. Clay Sc. 26, 337-350.
Wang, W., Rutqvist, J., Görke, U.-J., Birkholzer, J., Kolditz, O., 2011. Non-isothermal flow in low permeable porous media: a comparison of Richards' and two-phase flow approaches. Environmental Earth Sciences 62, 1197-1207.
Winterkorn, H.F., 1960. Behavior of moist soils in a thermal energy field. Clays and Clay Minerals 9, 85-103.
Yong, R.N., Pusch, R., Nakano, M., 2010. Containment of High-level Radioactive and Hazardous Solid Wastes with Clay Barriers. Spon Press, Oxford (UK).